DOI: 10.1002/adom.201900766

Article type: Progress Report

Photonic Memristor for Future Computing: A Perspective

Jing-Yu Mao, Li Zhou, Xiaojian Zhu, Ye Zhou and Su-Ting Han**

J.-Y. Mao, Prof. Y. Zhou

Institute for Advanced Study, Shenzhen University, Shenzhen, 518060, P. R. China

E-mail: yezhou@szu.edu.cn

Dr. L. Zhou, Prof. S.-T. Han

College of Electronic Science & Technology, Shenzhen University, Shenzhen, 518060, P. R. China

E-mail: sutinghan@szu.edu.cn

Dr. X. Zhu and Prof. S.-T. Han

Department of Electrical Engineering and Computer Science, University of Michigan, Ann Arbor, Michigan, 48105, USA

Keywords: photonic memristors, resistive switching, photonic computing, artificial synapses, neuromorphic computing

Abstract:

Photonic computing and neuromorphic computing could address the inherent limitations of traditional von Neumann architecture and gradually invalidate Moore's law. As photonics applications are capable of storing and processing data in an optical manner with unprecedented bandwidth and high speed, two-terminal photonic memristors with a remote optical control of resistive switching behaviors at defined wavelengths ensure the benefit of on-chip integration, low power consumption, multilevel data storage, and a large variation margin, suggesting promising advantages for both photonic and neuromorphic computing. Herein, the development of photonic memristors is reviewed, as well as their application in photonic computing and emulation on optogenetics-modulated artificial synapses. Different photoactive materials acting as both photosensing and storage media are discussed in terms of their optical-tunable memory behaviors and underlying resistive switching mechanism with consideration of photogating and photovoltaic effects. Moreover, light-involved logic operations, system-level integration and light-controlled artificial synaptic memristors along with improved learning tasks performance are presented. Furthermore, the challenges in the field are discussed, such as the lack of a comprehensive understanding of microscopic mechanisms under light illumination and a general constraint of inferior near-infrared (NIR) sensitivity.

1. Introduction

With the gradual failing of Moore's law and the constraint of the von Neumann bottleneck, a number of the revolutionary computing technologies, including photonic computing and neuromorphic computing, are exploited to fill the subsequent power vacuum. Following the theoretical concept of the "memristor" proposed by Leon Chua and the first physical demonstration in 2008,[1] rapid progress has been made in the growth of memristive devices.[2] The storage layer of

the memristor can be dynamically reconfigured under external stimuli, such as electric fields,[3] magnetic fields[4] or light illumination,[3] leading to variations in local conductivity and memory effects. The creation and annihilation of a conductive filament with either abrupt (binary) or gradual (analog) processes induce a wealth of device behaviors in this seemingly simple device, suggesting that the memristor holds great potential to facilitate the development of both photonic computing and biologically inspired computing.[5-10]

In general, photonics are capable of storing and processing data in an optical manner with unprecedented bandwidth and high speed.[11-14] Photonic computing utilizes on-chip optical interconnections to substitute electric wires in connecting memories, and central processing units (CPU) are proposed to mitigate the von Neumann bottleneck with low power consumption and high speed in data communication.[15-17] Two-terminal photonic memristors are able to be directly integrated onto processor chips, which subsequently improve the efficiency of the optical information shuttling.[18,19] On the other hand, with the failing of Moore's law, continuously scaling down to ensure integration of the increased number of memory cells is hindered by fabrication complexity and photolithography.[20,21] Exploring multilevel memristor cells with high storage density is an alternate method with the challenges shifting significantly to achieve separable states with high stability.[22] In photonic memristors, the light signal is employed as the extra terminal of the memristor devices to ensure a large memory window and variation margin of multiple storage levels.[23]

The human brain operates in a highly parallel and efficient fashion through a densely interconnected network of synapses and neurons.[24] The information transferred between the neurons is assisted by the synapses, which regulate their connection strength or synaptic plasticity to correspond to neural activities via chemical flux.[25,26] This plasticity is largely responsible for forming the basis of memory and learning inside the brain.[24] Motivated by the human brain, neuromorphic computing is expected to address the inherent limitations of conventional von Neumann architecture as well.[27] It is therefore indispensable to construct biorealistic synaptic elementary devices with rich spatiotemporal dynamics for the low power neuromorphic hardware.[28] In biological systems, utilizing light to modulate neural and synaptic functions, including activated/deactivated light-sensitive proteins, ion channels, agonists/antagonists, receptors, ion pumps, or ligands considered optogenetics, offers a higher degree of spatiotemporal resolution compared to traditional chemical and electrical approaches.[29-32] Inspired by the optogenetics, photonic memristors suggest an effective approach to modulate the synaptic plasticity for future neuromorphic computing as well.[33,34]

In this Progress Report, we focus on the recent advances in photonic memristors and their applications in photonic computing and optogenetics-tunable artificial synapses. Photonic memristors will be discussed in terms of light-involved physical mechanisms of photonic memristors, including the photovoltaic effect-mediated Schottky barrier, photovoltaic effect-induced formation/annihilation of conductive filaments, photogating effect, and photoinduced chemical reaction/conformation change. Additionally, the light-induced memory performance of photonic

memristors is presented. Light-involved functional systems integrated with memristors are also demonstrated to indicate novel photonic computing applications. Afterwards, optogenetics-tunable synaptic functions and neuromorphic systems emulated by photonic memristors are under discussion. In the end, we give a brief summary of the existing challenges hindering the development of light-involved applications and envision the future prospects of this novel physical modulation channel of light.

2. Physical mechanism of photonic memristors (resistive switching devices)

Normally, resistive switching (RS) devices are operated under electrical stimuli with binary resistance transitions between a high resistance state (HRS) and a low resistance state (LRS). In some cases, an intermediate resistance state (IRS) occurs, which involves multiple resistance states instead of two with an enhanced memory window or logic states for multilevel data storage. The resistance transition from HRS (LRS) to LRS (HRS) is defined as a SET (RESET) process, as shown in the middle part in Figure 1. In an RS memory device, the active materials (also known as switching medium) are sandwiched between the top and bottom electrodes to form a metal/insulator/metal (MIM) structure, implying its critical potential for the integration arrays with an ultrasmall device area (down to few nanometers), an ultrahigh density of scaled integration of memory elements, an extremely high switching speed, and low power consumption for the RS event. With various physical processes developing over time, the resistance changes occur in the form of either gradual or abrupt variations, suggesting rich behaviors with a seemingly simple structure.[35-37] It is worth noting that

the RS event is not only dependent on the active materials but also dominated by the choice of electrodes and the junction area at the interface between active materials and electrodes. Therefore, in consideration of the physical form of the conductive channel, the RS behaviors can be divided into two types, filamentary type and interface type, both of which are related to the physical reconfiguration of ion conditions via the redistribution of ions driven by an electric field.[38] As the most common type, filamentary-based RS behavior has features of highly localized and restricted filament shapes, resulting in the variation in the local resistivity and high current ratio (high LRS current) due to the formation of an extremely conductive filament bridging two electrodes.[39] Electrochemical metallization memristors (ECM) are associated with the switching behavior caused by the migration and redistribution of (active metal such as Cu and Ag) cations and redox reaction.[38,40] On account of the thin active layer, a high electric field is generated by a modest amount of applied voltage for the migration of ions while adjusting the ionic conformation within the active material serving as a solid dielectric electrolyte.[41] In addition, RS behavior in memristors may also stem from the conductive nanochannel formed by the growth and clustering of silver nanoparticles instead of charged ions, as was systematically studied and characterized by the Yang group.[26,42,43] For ECM, the severe challenge lies in the precise modulation of the morphology and controlled growth of metal filaments; additionally, high operation current must be addressed. Similar to ECM, valence change memristors (VCM) have the switching event driven by the movement and redistribution of internal ions, such as negatively charged oxygen ions (or positively charged oxygen vacancies) in oxides.[38,40] Nevertheless, the electrodes applied here are normally inert electrodes, such as Au or Pt, without electrochemical activity, and active species, such as oxygen

vacancies, play a dominant role in RS behavior. In addition, the reaction and gathering of oxygen vacancies at interfacial areas in the case of Ti or Al electrodes may also contribute to the RS operation.[44] Under an electric field, the device experiences a resistance transition from HRS, which results from the insulating property of stoichiometric oxides, to LRS as a conductive channel for electron transport formed by the field-assisted migration of oxygen vacancies. In stark contrast to oxides (or chalcogenides) used in ECM, the initially insulating near-stoichiometric oxides as active materials in VCM are involved in the chemical process to form nonstoichiometric products along with changes in the valance state of the metal element after RS operation. Furthermore, the generation of oxygen vacancies may give rise to the deformation of oxides and increasing amounts of trap sites (defects) for charge carriers that also lead to the trap-mediated switching event. The major problem for VCM is the operation stability, since repeated switching cycles may lead to the deterioration of reliability.

The microscopic mechanism of the RS under light illumination becomes more complicated when taking photovoltaic, photogating effects and photoinduced chemical reactions into consideration when the fundamental operation mechanism is reliant on the electrically induced dynamic motions mentioned above. With the incoming light, RS memory parameters no longer stay the same, where the operation current, including I_{HRS} and I_{LRS}, and SET/RESET voltages can be properly tuned depending on the wavelength and the intensity of light. Moreover, RS under the light application of limiting conditions possesses the virtue of diversified operation modes, encompassing photoinduced SET or RESET operations as well as a change in memory type. Hence, RS in photonic memristors,

regarding the operation modes, can be sorted into photoassisted and photoinduced processes (transitions), both of which are strongly connected with ionic dynamics. Accordingly, the choice of active materials and junctions at interfaces for RS events is of critical importance since they work as switching media to be modulated not only by electrical signals but also by incident light, which is considered to be an additional dimension for specific control of RS behavior. To do that, light, as an effective means, is supposed to achieve deep engagement in ionic reconfiguration across the dielectric active layer and the interfacial region or endure photoinduced chemical reactions where new products are formed with distinct electrical characteristics. Beyond that, another important implementation for effective control of RS behavior is believed to be the photogating effect by means of electrostatic force (potential), which is rarely reported relating to RS behavior.[45] Slightly different from that of the electrically induced RS memory, the physical mechanisms of photonic memristors with respect to the effect of light are classified into four categories, depicted in Figure 1, including the photovoltaic effect-mediated Schottky barrier, photovoltaic effect-induced formation/annihilation of conductive filaments, photogating effect, and photoinduced chemical reaction/conformation changes, as discussed in detail in the following.

2.1. Photovoltaic effect-mediated Schottky barrier

The photovoltaic effect typically involves the separation of photogenerated electron-hole pairs, the creation of free carriers, and the production of an electrical voltage or current from incident photons.[46] Photovoltaic materials are supposed to possess traits, such as efficient light harvesting and large absorption coefficients, which allow full absorption of photons with energy above their

bandgap and impeds the undesired charge recombination, a sufficient exciton diffusion length to ensure the efficient charge and voltage generation. The electron-hole separation is highly related to the internal electric field induced by the heterojunction interface (heterojunction system) or by the Schottky barrier between the semiconductor and metal,[47] which leads to a movement of holes towards the positive electrode and electrons towards the negative electrode, followed by the extraction of charges to external circuits and the generation of the open-circuit voltage. Therefore, the devices based on photovoltaic effects were applied in field-effect transistors, where the extended light detection range, high gain and bandwidth have been achieved, which can then be extended to the memristor application.[48] The photovoltaic effect induced excitons can be separated at the interfaces between electrodes and active materials (single component) or at the interfaces between different components (hybrid system), contributing to ion migration or carrier trapping to tune the interfacial barrier critical for RS behavior.

In the migration of ions, such as positively charged oxygen vacancies, diffusion in oxides has been demonstrated with the capability of modulating the energy barrier in the depletion region, which may induce persistent photoconductivity under light illumination. The interfacial barrier between the electrode (ITO) and active materials can be lowered by the photovoltaic effect. Li et al. demonstrated an optically programmable and electrically erasable memristor with a simple structure of ITO/CeO_{2-x}/AlO_y/Al, which can be labeled as the photoinduced SET process.[11,23] CeO_{2-x} was carefully chosen to act as a photoactive material with a wide range of photoresponses attributed to the defect energy level embedded in the bandgap as well as an active material for RS

events due to the nonstoichiometric nature and was beneficial for the easy formation of a native AlO_y layer as a thin Schottky junction to induce an insulating barrier, which suppresses the leakage current while the stable interfacial trapping sites can be created. During positive voltage sweeps (electrical mode), additional positively charged oxygen vacancies were attracted towards AlO_y, leaving electrons driven towards the ITO electrode under the electric field. The accumulation of oxygen vacancies at the CeO_{2-x}/AlO_y interface results in a thinner Schottky barrier; thus, the resistance changes from HRS to a low resistance state. Upon the introduction of light, the optical programming was achieved, which stems from the narrower junction barrier and reduced junction resistance that subsequently enhanced charge transport at the interface by the diffusion of photoexcited electrons away from the interfacial region with the accumulation of more oxygen vacancies in the opposite direction, as shown in **Figure 2**a.[8,11] In addition, the multilevel nonvolatile state was realized by the modulation of light intensity and wavelength, implying a possible application in future high-density optoelectronic memory.[18] The ITO/Nb:$SrTiO_3$ heterojunction also shows an analogous phenomenon that was reported by the same group in 2019.[49] Similarly, the high photosensitivity of the Nb:$SrTiO_3$ and ZnO nanorods heterojunction ensures the versatile reconfiguration of ionized oxygen vacancies and the alteration of the effective energy barrier in the interfacial region under the optical stimuli (Figure 2b).[44,50] Multiple oxide materials have been employed as the active materials for memristors under electrical and optical stimuli, exhibiting multilevel data storage.[22,51] The generation of oxygen vacancies and the tuning of the Schottky junction at the interfaces ($SrTiO_3$) can improve the RS behaviors by introducing multiple resistance states and lowering operation voltage under the application of light.[23,50,52]

Perovskite materials have attracted enormous attention due to their extraordinary broadband light absorption and high bandgap tenability. In addition to their potential application in next-generation solar cells and light-emitting diodes, the dynamic ion migration and ferroelectric behavior related to current-voltage hysteresis have been considered the basic form for data storage, although they are not preferred in photovoltaic applications.[47] For perovskite-based memristors, the interfacial barrier can be readily modulated by photovoltaic effect-induced ion migration.[53] Huang et al. discovered the switchable photovoltaic effect in perovskite optoelectronic devices. The perovskite device with symmetric structure (Au electrodes) transformed from a neutral state to a p-i-n junction with obvious variation in open-circuit voltage (V_{OC}) and photocurrent.[47] Importantly, the memristive hysteresis was mainly attributed to the charge accumulation induced by negatively charged Pb and MA vacancies and positively charged I vacancy migration, resulting in p- and n-type doping at perovskite/PEDOT:PSS and perovskite/Au interfaces, respectively (Figure 2c). Conversely, the perovskite memristors can be read out in two modes by both electricity (current on/off ratio of approximately 10^3) and light (different V_{OC}). Wu et al. systematically studied the switching mechanism of hybrid perovskites $CH_3NH_3PbBr_3$ ($MAPbBr_3$).[54] By tuning the maximum positive/negative voltage during sweeping, various degrees of hysteresis were addressed, which originated from the modulation of the perovskite/ITO Schottky junction through the migration of charged ions/defects (MA vacancies). Since perovskite materials exhibit impressive photoresponse, light signals were also employed for the involvement of tuning the perovskite-based memristors, where UV illumination gave rise to multilevel data storage and the photocurrent increased at both HRS and LRS (Figure 2d). More obvious current variation was observed for HRS, indicating a thicker

depletion region in this scenario. The overall enhancement in current was due to the neutralization of charged ions with additional photogenerated charge carriers at the interfacial region, while interface-based switching (tuning perovskite/ITO Schottky barrier height) was responsible for RS operation when the possibility of metallic filament formation was excluded.

2.2. Photovoltaic effect-induced formation/annihilation of conductive filaments

For cation memristors, active metal electrodes, such as Cu or Ag, are often chosen as anodes for the purpose of redox reactions (ECM), while in anion memristors, the formation and annihilation of anion conductive filaments is the main mechanism for RS.[55] Upon the application of external electric fields, conductive filaments are formed via the migration of either charged ions or vacancies (electrical SET process), whereas light has not been reported to accelerate this process. In contrast, light-assisted diffusion of charged ions was proved to facilitate the RESET process. As discussed above, ion migration inside lead halide perovskite results in the variation of the interfacial barrier that further influences the RS behavior. In addition, filamentary RS involving either Ag or halide ion migration was also proposed as the switching mechanism of recently reported halide perovskite-based memristors, depending on the selection of electrodes. Lu et al. reported the RS effect based on $MAPbI_3$ with tunable SET/RESET voltages,[56] owing to the formation and rupture of conductive channels consisting of iodine vacancies (Figure 2e). In $MAPbI_3$, both I^- and MA^+ ions have been confirmed capable of migrating while the diffusion of I^- is preferable to induce RS due to the lower diffusion energy barrier.[57] However, with visible light illumination, the filaments composed of

iodine vacancies became unsteady and tended to rupture, arising from the spontaneous diffusion and recombination of iodine vacancies with iodine ions, which leads to a photoinduced RESET process. Figure 2f depicts the light intensity effect on the RESET voltages of the $MAPbI_3$ device with a planar structure. An obvious increase in the SET voltage and decrease in the RESET voltage can be observed with increased light intensities. The coupling of electrical and optical effects resulted in the implementation of an electrical-SET and photoinduced RESET memory cell with an ultrahigh on/off ratio and the ability to remotely measure the device conductance. Later, a memristor with the analogous function had been realized in a doped inorganic perovskite material system (Ti-doped $BiFeO_3$) based on ferroelectric photovoltaic effects,[50] in which the redistribution of electrons and atomic partial densities of states in the $BiFeO_3$ film caused by Ti doping can improve the photovoltaic effect and induce the filament formation. The ferroelectric photovoltaic V_{OC} was properly modulated by RS behavior in Ti-doped BFO film. Thus, the electric-optical memory can be operated in the form of electrically induced resistance switching between HRS and LRS and optical reading of the V_{OC} at different resistance states.

Similarly, Han et al. reported a near-infrared (NIR) controlled memristor that can induce unusual RESET operations under 790 nm NIR illumination.[58] After the SET process, in which Ag conductive filaments were formed to bridge the top and bottom electrodes, photogenerated electrons were arrested by the $MoSe_2/Bi_2Se_3$ hybrid layer, leaving untrapped holes that rendered the oxidation reaction of Ag clusters to Ag^+ cations. Gradual oxidation of Ag atoms within conductive filaments

results in photovoltaic effect induced annihilation of the Ag conductive filaments operation in the form of a current decline of the RS device.

2.3. Photogating effect

Photogating effect, literally defined as resistance modulation through a light-induced electric field, is widely used in photodetectors or transistor-based flash memories. When photogenerated charge carriers (e.g., holes) are trapped in localized defects or trapping layers, the introduction of a trapped holes-induced electric field gives rise to more electrons in the conductive channel, thus inducing the increase in channel conductance.[59] The electrostatic force induced by trapped charge carriers contributes to the modulation of the charge transport along the conductive channel by means of either an electrical or a light signal. Thus, it will be intriguing as well as challenging to develop optical memory devices on the basis of the photogating effect. 2D van der Waals (vdWs) materials, especially the heterostructures, have aroused remarkable interest in photonic memories and synaptic devices for neuromorphic computing due to their intriguing optoelectronic and mechanical properties.[37,60-63] In recent years, flash memories based on the 2D vdWs heterostructures exhibit highly competitive performance with a large memory window, high on-off current ratio and long retention time.[64,65] However, the complexity of the three-terminal structure hinders the variability, expansibility and integration density of the memory device for further development. Lee et al. presented a two-terminal tunneling random access memory (TRAM) device based on a 2D graphene/h-BN/MoS_2 heterojunction, analogous to the device structure of flash memory, in which the major discrepancy yields the number of terminals to modulate the device

performance.[45] Graphene with a proper thickness of h-BN and MoS_2 is used as the floating gate, tunneling insulating layer and semiconductor material. TRAM, which displays a simplified device structure that acts as a memory device that converts from a three-terminal flash memory structure to a two-terminal configuration, exhibited a reduced complexity with an ultralow off-state current of 10^{-14} A and ultrahigh write/erase current ratio of 10^9. In terms of the operation mechanism of the TRAM, the charge carriers can tunnel through the insulating h-BN layer and maintain the highly conductive graphene layer under the large electric potential between the drain electrode and the floating gate, which cannot tunnel through the h-BN layer away from the floating gate to the source electrode due to the limited potential difference, thereby achieving the storage of charge carriers. TRAM also presented excellent durability over 10^5 cycles and superb stretchability with no obvious device performance degradation changes up to 19% strain, resulting from the superior mechanical stability of the 2D materials assembly. Recently, on the basis of previous work, they developed a multilevel nonvolatile optical memory based on the MoS_2/h-BN/graphene heterostructure, where the MoS_2 monolayer acts as both photoactive and semiconductor material.[66] The 2D material heterostructure-based optical TRAM device also exhibited an ultralow off-state current of 10^{-14} A and a significant current increase was induced by laser light illumination, leading to nonvolatile memory behavior shown in **Figure 3**a. Reproducible electrical programming and light erasing operations were carried out (Figure 3b). Under light illumination, the photogenerated holes in MoS_2 can easily tunnel through h-BN to the graphene layer, neutralizing the stored electrons and enabling the optical erasing operation (Figure 3c). The optical-tunable TRAM revealed robust memory performance, such as an ultrahigh current on/off ratio over 10^6, stable endurance over 10^4 cycles, a

long retention time over 10^4 s and multilevel storage (four-bit). Therefore, the optical TRAM opens up a promising strategy for high-density integration of novel multifunctional optoelectronic devices with 2D vdWs heterostructures.

Recently, Han et al. carried out the investigations on the effect of incident light with different wavelengths and intensities on RS characteristics and the underlying mechanism of light-tunable memory devices based on quantum dots (QDs), which are widely used and studied for their quantum confinement effect, including $CsPbBr_3$ QDs and carbon QDs-silk protein bicomponent blend.[67,68] In both cases, with the application of UV light, SET and RESET voltages were effectively reduced, facilitating the development of energy-efficient memory. After light absorption, photogenerated electron-hole pairs at the interfaces were separated into electrons and holes that were driven to the anode and cathode, respectively. Along with the externally injected charge carriers, photogenerated charge carriers were also trapped inside the QDs, leading to the photogating effect, which further accelerated the formation of the conduction path as well as the decreased voltage required for the resistance transition. To confirm the charge trapping behavior within the QDs, in situ Kelvin probe force microscopy (KPFM) measurements were carried out. The increase in potential difference with QDs and further enhancement under UV light illumination after carrier injections from the conductive tip confirmed the feasibility of light-tunable memory characteristics and was accounted for in the modulation of charge trapping ability within QDs (photogating effect). These works emphasize the importance of the development of light-tunable memory devices based on QDs and other materials.[69]

Most light-tunable memristors require the application of high energy UV or visible photons, whereas NIR photonic memristors have rarely been reported.[62,70] Upconversion materials have excellent photoluminescent properties that can absorb long-wavelength light and radiate light with higher energy.[70] Heterostructures combining upconversion materials with 2D materials can provide a novel way of light modulation in the RS process, contributing to enhanced photo energy utilization and photosensitivity. Han et al. integrated directly grown MoS_2-$NaYF_4$:Yb^{3+}, Er^{3+} upconversion nanoparticle (UCNP) nanocomposites into memristors, in which MoS_2 nanosheets could absorb the visible light emitted from the UCNPs when excited by NIR illumination.[62] In material characterizations, ideal matches were found between the absorption peaks of MoS_2 and emission peaks of UCNPs under 980 nm NIR irradiation, resulting in efficient nonradiative energy transfer from UCNPs to MoS_2. An evident decreasing trend was found for SET and RESET voltages of light-controllable MoS_2-UCNP nanocomposite memory devices, while current at LRS increased drastically under NIR irradiation, which can be extended to diverse resistance levels (at different NIR intensities). Moreover, conductive atomic force microscopy (C-AFM) mapping measurements as well as the well-fitted space charge limited current (SCLC) model were exploited to explain the underlying mechanism of tunable charge trapping endowed by MoS_2. Upon the application of NIR irradiation, excitons were generated in UCNPs followed by the rapid charge carrier separation at the MoS_2–UCNPs interface that further led to charge trapped in MoS_2 and photogating accelerated SCLC. This study paves the way towards the modulation of NIR memory behavior and provides insight into further light-controlled encrypted data storage using invisible light illumination.

2.4. Photoinduced chemical reaction/conformation change

Photoinduced chemical reactions have attracted increasing attention in many promising applications such as energy conversion and environmental safety due to their atom-economy (only photons are needed) and low energy consumption (depending weakly on temperature).[71] High selectivity of a photoinduced chemical reaction is achieved originating from the adjustable photon energies and fast electron transfer. Photoinduced chemical reactions involve the absorption of photons to render the molecules excited and induce the chemical changes such as ionization and isomerization.[72] Additionally, the electrical properties, such as the energy bandgap and dipole moment of small molecules, can be precisely manipulated by the photoinduced ionization and isomerization, resulting in the optimization of RS behavior in optical memristors. In RS memory, light-induced transformation between switching behaviors is strongly related to conformation change within the photoactive materials, which may lead to the change in chemical bonding and energy band.

Reduced graphene oxide (rGO) has attracted remarkable interests due to its advantages of tunable bandgap, proper electrical properties, and large-scale synthesis, as well as its application in nonvolatile RS.[36] Han et al. demonstrated a phototunable memristor based on ITO/phosphotungstic acid (PW)/graphene oxide (GO)/Al structure.[73] PW can act as a multifunctional catalyzer to reduce GO under UV irradiation and induce the transition of memory types from WORM to bipolar RS. The irreversible transformation in RS behavior is due to the discrepancy in the energy level between GO and rGO, as well as the decreased interface energy barrier in the PW/rGO junction. Zhao et al.

proposed a photocatalytic reduction method via the introduction of TiO_2 into GO, which provided the desired control of rGO-domains.[74] A significantly improved performance of Al/GO-TiO_2/ITO memory was observed after photocatalytic reduction of GO, presenting a reduced SET voltage (from 2.1 V to 0.52 V) without the electrical forming process. Increased photoreduction time as well as the concentration of TiO_2 can lead to the generation of local rGO-domains through controlled photoreduction. In addition, this method allows low temperature and solution process of high-performance memristors on flexible substrates.

Organic molecules with functional donor and acceptor groups are artificially tailored to achieve intramolecular charge transfer between these groups.[75,76] By means of deliberate control of the functional groups (mostly acceptors), multilevel resistance states can be clearly realized arising from the charge transfer from a donor to multiple acceptors.[77-80] Ye et al. reported a meta-conjugated donor-bridge acceptor (DBA) molecule as the RS media to achieve ternary states storage with the help of UV stimuli, which originates from the charge transfer from triphenylamine (donor) to 2-dicyanomethylen-3-cyano-4,5,5-trimethyl-2,5-dihydrofuran (acceptor) (Figure 3d).[81] Additionally, the UV−vis spectra provided crucial information on the UV-assisted step-by-step oxidation based on the extent of bathochromic-shift of the absorption peak at long wavelengths. The cooperative effect of both redox systems of the organic small molecules and the assistance of UV ensures the effective modulation on the optoelectrical memory device with multilevel storage.[82]

As a well-established class of photochromic molecules, the isomerization between two structural conformations in diarylethene (DAE) molecules can be induced via optical irradiation, and

the material properties of the isomers can be changed with the external optical stimulus.[47,83,84] The significant variations in the highest occupied molecular orbital (HOMO) and lowest unoccupied molecular orbital (LUMO) energies as well as the dipole moment make them promising candidates as the active material in optoelectronic devices. Ling et al. demonstrated a reversible RS characteristic in a DAE-type molecule, named BMThCE, upon UV or visible light irradiation.[85] The device demonstrated WORM characteristics when the BMThCE molecule was in a ring-open state (o-BMThCE) under visible light, which could then change to the c-BMThCE (ring-close state) under UV irradiation (Figure 3e), resulting in an erasable nonvolatile bipolar RS characteristic (Figure 3f). In consequence, the discrepancies in RS characteristics originated from the tunable HOMO/LUMO of BMThCE under different wavelengths of light irradiation. The HOMO of o-BMThCE is lower than that of c-BMThCE. Therefore, the deeper hole trapping in the o-BMThCE compared to c-BMThCE occurred. It can be briefly concluded that light-induced transformation between conformational structures with a change in energy level indeed has a pronounced impact on the RS types, which greatly modulates the device performance in an accurate and energy-efficient way.

3. Photonic memristor for future photonic computing

3.1. Light-involved logic operations

Memory devices such as conventional transistor-based flash have their intrinsic and fixed function to store information. By designing memristors capable of storing while processing information based on incident signals, logic operations can then be performed in a highly parallel and energy-efficient way. Novel light-modulated two-terminal memristor devices operating as data storage with the

ability to conduct logic operations with simple device configuration is drawing great research attention since logic plays a fundamental role in the binary system and the introduction of light brings an ingenious approach to merge electric signals with the additional dimension of light.[86] Apart from the tunable memory characteristics of the photonic memristors we discussed above, novel memory integrated with other functions, including arithmetic and demodulation, is a fundamental basis for future in-memory computing using electrical and optical signals as inputs. Two light sources, blue and green lights, along with wavelength and light intensity were capable of realizing four memory states, enabling the information storage and transmission of 8-bit codes in ITO/CeO_{2-x}/AlO_y/Al devices in which the physical mechanism was discussed earlier.[23] Upon the basis of the linear dependency of photocurrent on the number of applied optical pulses, arithmetic operations including "Counter" and "Adder" were hence implemented. The simple integration of memory and logic functions offers a feasible route to reduce system complexity in the integrated circuits.[87,88] In addition to basic nonvolatile memory and arithmetic function, as well as the light-induced RS effect, memlogic devices with arithmetic functions were also proposed by Li et al. The device can operate as a light-controlled logic gate, which implements fundamental Boolean logic including the "AND", "OR", and "NOT" operations by means of controlling the charge trapping at the CeO_{2-x}/AlO_y/Al interface.[11] Both electrical and light pulses are termed as logic input while device current is considered an output of the logic gate. When the output current exceeds a given threshold value, such as in the case where the light pulse is applied along with the voltage pulse, logic "1" is achieved. If no or either stimulus is applied, the output is logic "0," realizing the "AND" function. In addition, "OR" and "NOT" functions can be implemented by preprograming the device to an

intermediate resistance state and adding an additional RESET electrical pulse. **Figure 4**a demonstrates the input of two patterns to the memlogic array as an image processor and are recognized together with memory characteristics that were validated to implement SAME FINDER and ALL_FINDER functions (Figure 4b and 4c). Furthermore, the parallel operation of data recording and processing inside a single memory cell as well as the reconfigurable logic operations indicate a promising potential in future in-memory computing.

3.2. System-level integration of a photonic memristor

The human visual system allows for the collection, transportation and processing of visual information from ambient objects. To simplify these processes, photodetectors can be regarded as retinas to sense the light signal and then transform the light signal into an electrical one to be processed and recorded in memory devices.[89,90] Chen et al. reported a novel combination of In_2O_3-based image sensors and Al_2O_3-based memristors, which constructed artificial visual memory motivated by UV light for the application of image sensing and storage.[91] The visual memory system could be operated by excellent detection of UV light while the information was recorded in the memristors. Figure 4d demonstrates the configuration of visual memory, where the image sensor and memory unit are connected in series with a conjunct electrode. When the UV light is applied, the resistance decrease of image sensors leads to the increase in partial voltage on the memristors, thus switching the memory device from HRS to LRS. Once the light illumination is removed, the recorded image shows a long retention time of more than a week to be recognized, and the stored information can be RESET via a reverse voltage (Figure 4e). The obtained results signify the potential

application of visual memory systems in the development of artificial electronic eyes and bioinspired systems.[92] In 2016, Kim et al. presented a photodestructible memristor based on modified UCNPs.[93] The broadened absorption range for the modified UCNPs to a visible range by introducing multiple fluorescent dyes extends the choice of light source, enabling the erasure of specific information that is locally stored inside the memory device. Figure 4f and 4g depict the destruction of selective regions by light illumination at a wavelength of 800 nm only, which provides insight into data security applications as an invisible light signal is a fascinating candidate for information manipulation.[94] Memristors with integrated functions, including light detection, data storage, and in-memory computing, are primary steps towards complex artificial neural networks. The abovementioned photonic memristors are beneficial to the construction of optoelectronic synaptic devices, which come with advantages in novel optical communications.

4. Photonic memristor for optogenetics-tunable neuromorphic computing

In contrast to conventional digital computers based on the von Neumann architecture, where the memory is separated from the central processing unit, the human brain has tens of billions of neurons connected to each other in a vast network with the synapses.[35,95] In this system, a great deal of information is transmitted all the time, constituting our memory, logical reasoning, linguistic competence and visual-spatial cognition. In a single neuron, information is transmitted by electrical signals. The electric potentials inside and outside the cell membrane are reversed with signal conduction and followed by a large amount of calcium ion influx. The traditional method for

neuroscientists to activate a nerve cell is with electrical stimulation (electrode placed near a neuron to change its electrical potential) or the chemical approach (apply small molecules that act as neurotransmitters to the cell receptors). However, electrical stimulation cannot accurately localize the cell, while chemicals cannot provide accurate time control due to their slow release. Therefore, the development of unique and reliable techniques that are able to control neuronal activity with precise temporal and spatial precision is highly desirable.

In recent years, a new technology, termed “optogenetics”, which uses external light stimulation to control the behavior and function of neuron cells with high specificity, has been developed, and its temporal resolution has been extensively utilized in neuroscience.[96,97] In optogenetics, light is employed to activate/deactivate the light-sensitive ion channels and change the membrane potential on both sides of the cell membrane. Thus, the excitation or inhibition manipulation of the neuron cell can be achieved. The basic principle of optogenetics is shown in **Figure 5**a.[29,30] Photosensitive membrane channel proteins, such as channelrhodopsin (ChR2) and Halorhodopsin (NpHR), are transferred into neuron cells for ion channel expression. In the case of ChR2, when a neuron cell is exposed to a blue laser at 470 nm, a cationic channel of neurons opens, allowing a large number of cations (such as Na^+ and Ca^{2+}) to flow into the cell. The action will depolarize the neuronal membrane and positively modulate the action potentials, thus placing the neuron in an excited state. For NpHR, when a neuron cell is exposed to a yellow laser at 580 nm, the anion (Cl^-) is allowed to enter the cell through the ion pump, inducing the membrane hyperpolarization and negatively modulating the action potentials, thereby inhibiting the neuron.

In biological systems, calcium ions (Ca^{2+}) play an important role in many physiological processes, such as intracellular information transmission, gene expression, neurotransmitter release and so on. Benefitting from the optogenetics technology, it was recently demonstrated that light can activate/deactivate the Ca^{2+} channels to modulate the synaptic plasticity of mice.[98] It is noted that the memristors resemble typical biological synapses in both structure and kinetic processes. The current change in the memristor stimulated by voltage pulses resembles the Ca^{2+} dynamics in biological counterparts during the modulation of synaptic plasticity.[99,100] Thus, the strategy of using light as an external stimulus to modulate synaptic plasticity in memristors is a feasible method to emulate optogenetics-mediated synaptic functions.

Memristors, as artificial synapses, are termed RS devices, of which the present resistance state is closely related to the voltage stimuli that were previously applied and can be well-tuned with analog switching characteristics extensively studied to emulate biological synapses functions with only electrical input.[101,102] Photonic memristors open up novel access for the modulation of synaptic weight by light for further transmission and processing of stimulus information (Figure 5b).[103] Very recently, light acting as a noninvasive synaptic modulator that is physically separated from the conductive channel can also effectively and energy-efficiently tune the synaptic functions of photonic memristors based on photoactive materials.[104] On-chip photonic computing has been proposed as an alternative to replace the electronic computers to eliminate the von Neumann bottleneck with high speed and low power consumption in data transmission.[105] Phase-change materials (PCMs) have emerged as viable materials for nonvolatile photonic memories due to their

distinct deference in optical and electrical properties between their amorphous and crystalline states.[106] In another aspect, the promising fast processing ability of PCMs make it a potential candidate for photonic neuromorphic systems.

Recent works by Cheng et al. demonstrated an on-chip photonic synapse with PCMs incorporated into a tapered waveguide structure.[15] Based on the rationally designed structure, the photonic synapse shows an ultrahomogeneous electric field distribution. Therefore, the synaptic weight of the photonic synapse can be simply and effectively controlled by varying the pulse numbers sent down the waveguide while retaining the pulse duration and energy. Synaptic plasticity, including the spike-time-dependent-plasticity, can be mimicked via an all-optical method. This work provided a simple but powerful approach to realize a low power consumption artificial photonic synapse, which may establish a prototype for future large-scale photonic neuromorphic networks. Purely photonic triggered memory or artificial synapse can be implemented via waveguide structures, while for electrical-controlled synaptic devices, the light signal offers a novel approach to nondestructively modulate the synaptic weight of the conductive channel by a spatially separated stimulus.[17] In addition, more superiorities, such as separated learning and readout operations, broadband response to light illumination and significantly lowered energy consumption, open up encouraging prospects for future neuromorphic computing. Two-terminal oxide heterojunction-based memristors including ZnO_{1-x}/AlO_y, In_2O_3/ZnO and ITO/Nb:$SrTiO_3$ were also reported to emulate multiple fundamental synaptic functions, including STP, LTP along with phototunable excitatory postsynaptic current (EPSC) and paired-pulse facilitation (PPF), and were

faithfully emulated by optical stimuli (Figure 5c and 5d).[49,107,108] Similarly, current-voltage characteristics were attributed to the intrinsic charge trapping capability inside the oxide heterojunction and led to a nonvolatile persistent photocurrent, which is a vital element to realize light-induced LTP behavior. Moreover, other photoactive materials, such as perovskite and two-dimensional semiconductors, also possess the ability to truly emulate the synaptic behaviors of biological synapses using light as the input to modulate synaptic weight.[16,109-112] Different from two-terminal memristors, three-terminal synaptic transistors, especially light-gated synaptic transistors, demonstrate tunable synaptic behaviors through controllable charge trapping and detrapping at interfaces or trap sites; inherent photoconductivity (PPC)[113-116] also emerged as a promising optoelectronic device for modulating synaptic weight in an energy-efficient way.[103,117] Recently, light-stimulated synaptic transistors based on inorganic perovskite quantum dots (C_SPbBr_3 QDs) and organic semiconductors exhibited excellent photoresponsivity and delayed the decay process of the photocurrent and synaptic tunability due to the efficient charge separation of photogenerated excitons.[118,119] Therefore, neuromorphic potentiation and depression were effectively conducted by photonic and electrical stimuli. These works implemented the basic synaptic functions by applying an external light signal and provided a potentially solid strategy for the development of novel low-power neuromorphic computing systems and artificial neural networks.[16,120]

As we mentioned in the previous section, $MAPbI_3$-based memristors exhibited light-tunable SET/RESET voltages attributed to the formation and annihilation of the conductive channel

composed of iodine vacancies.[34] Recently, inspired by the manipulation of neuronal activities of optogenetics beyond conventional means, Lu et al. exploited a light-modulated $MAPbI_3$-based two-terminal memristor device as an artificial synapse for the purpose of simulating fundamental synaptic behaviors in biological neuronal systems.[34] Enlightened by the tuning of the Ca^{2+} dynamics, light can be considered an additional source to modulate the connection strength of the conductive channel. Light illumination applied to the planar channel induces the suppression of iodine vacancies and facilitates the relaxation process of device conductance, authentically emulating the synaptic behavior of biological synapses. Furthermore, the strengthening and weakening of the conductive channel induced by the adjustment of different incident light parameters displays significant resemblance to the memory and forgetting processes.

Inspired by light-excited secretion of dopamine (neurotransmitter) and the promotion of fast learning and adaption of neural activities, computing systems capable of rapid learning and recognition can be designed at an extremely low power-consuming level. The light-involved tuning of synaptic weight enables a significant reduction in energy consumption as well as processing time. In 2018, a two-terminal light-assisted artificial synapse with improved synaptic plasticity was proposed by Ham et al.[121] Light illumination facilitated the iodine vacancies movement in the perovskite layer, leading to easier realization of long-term potentiation when combined with electrical input signals, which resembles the phenomenon of dopamine-assisted behaviors in biological synapses. A pattern “3” was input into a single-layer neural network composed of 784 input and 10 output neurons between which are individual synapses with different synaptic weight

for recognition (Figure 5e). Each input neuron corresponds to a pixel of the input pattern. After updating the weight, the fully trained artificial network is able to execute the recognition process of input patterns. It is noteworthy that the perovskite-based synaptic memristor demonstrated good learning capability and acquired a high pattern recognition rate of 81.8% after limited learning phases with light illumination while consuming much less energy than that of only electrical input (Figure 5f and 5g). A similar training process and resulting conclusion can also be drawn for photosynaptic transistor devices based on charge trapping/detrapping.[103] To summarize, light involved operations demonstrate improved data storage and synaptic behaviors with the potential for building multidimensional neural networks.[21,103,122] The massless and uncharged nature of photons can avoid the charge-based wiring issue and allow it to perform efficient communication performance.[123] It is highly promising to use light instead of electrical signals for communication in artificial neural networks due to the parallel computing capability and power efficiency of optical systems.[124] Recently, Shen et al. demonstrated a fully optical on-chip implementation of neural networks where the computational speed and power efficiency can be enhanced by the coherent and linear-optics matrix multiplication.[14] This work lays a solid foundation for the realization of a truly integrated all-photonic neuromorphic system based on all-photonic artificial synapses to perform ultrafast neuromorphic computations.

Bioinspired nervous systems with sensory, integrative and motor functions have turned into a core technology for next-generation electronic neurorobotics in the booming artificial intelligence industry.[125-127] This requires that the sensory receptor has hypersensitive sensing of the changes in

the external environment, the sensing system has a strong analyzing and interpreting ability of the sensory information to allow appropriate responses and proper decision making, and the motor unit has an accurate response to the sensory information. Recently, Lee et al. demonstrated the first optoelectronic nervous system based on an organic artificial sensory synapse and a neuromuscular system (Figure 5h).[125] The ion gel-gated stretchable organic nanowire synaptic transistor (s-ONWST) can mimic typical short-term synaptic plasticity, including EPSC, PPF, spike-dependent plasticity (the verified parameters including voltage, number, duration and frequency) and high-pass filtering, at both 0 and 100% strains. Additionally, by combining with an organic photovoltaic device, the s-ONWST can convert the light signals into electrical presynaptic spikes to cause postsynaptic potentiation of the artificial synapse. More importantly, this organic optoelectronic synapse can actuate an artificial neuro-muscle to display the analogous biological muscular contraction mechanism, which is difficult to realize in conventional artificial muscle actuators. This work would suggest a promising strategy for the development of movement systems in neurologically inspired robotics.

5. Summary and outlook

In summary, inspired by the improved data communication speed of fiber optics and the high parallelism of optogenetics-tunable biological synapses, photonic memristors with on-chip integration offer a promising approach to develop future computing systems past the Moore's law and von Neumann era. Photonic memristors and their applications in photonic memory and

computing functions were discussed in detail with regard to the physical mechanism. Emulation on optogenetics-modulated artificial synapses and further artificial neural networks with light-tunable and enhanced synaptic behaviors were presented. Moreover, light-involved logic operations, system-level integration and light-controlled artificial synaptic memristors along with improved learning tasks performance were presented. However, compared with traditional CMOS technology, photonic memristor applications are very straightforward, though many challenges remain. The most important challenge is the lack of comprehensive understanding of the microscopic mechanism of the RS under light illumination, since the operation principle is more complicated by considering photovoltaic and photogating effects. In addition, there remains a vacancy in RS behavior in view of both the increase and decrease in resistance of optoelectronic memristors by means of complete light control. Moreover, requirements on the broadband response or specific narrow wavelength response can vary significantly depending on the applications. A general constraint in the photonic memristors lies in their inferior IR sensitivity as opposed to their UV-visible sensitivity, making the broadband absorption and discrimination between the signals of different wavelength difficult. Thus, the energy band optimization and the effects limiting the optical-electrical conversion need to be elucidated. Finally, technique issues, such as employing transparent electrodes instead of opaque metals and integrating light sources with photonic memristors, should be addressed. Creative and multidiscipline research, including chemistry, physics, electrical engineering, computer science and neuroscience, is needed to eventually apply photonic memristors in novel photonic and neuromorphic computing systems.

Acknowledgements

J. Y. M. and L. Z. and contributed equally to this work. The authors thank Mr. Junhong Li for his kind help in the manuscript writing. The authors acknowledge the grants from Natural Science Foundation of China (Grant Nos. 61601305 and 61604097), Guangdong Province Special Support Plan for High-Level Talents (Grant No. 2017TQ04X082), Guangdong Provincial Department of Science and Technology (Grant No. 2018B030306028), the Science and Technology Innovation Commission of Shenzhen (Grant Nos. JCYJ20180507182042530, JCYJ20180507182000722, JCYJ20170818143618288 and JCYJ20180305125314948), Shenzhen Peacock Technological Innovation Project (Grant Nos. KQJSCX20170727100433270 and KQJSCX20170327150812967), NTUT-SZU Joint Research Program (Grant No. 2019006) and the Natural Science Foundation of SZU.

Received: ((will be filled in by the editorial staff))
Revised: ((will be filled in by the editorial staff))
Published online: ((will be filled in by the editorial staff))

References

[1] D. B. Strukov, G. S. Snider, D. R. Stewart, R. S. Williams, *Nature* **2008**, *453*, 80.

[2] J. J. Yang, D. B. Strukov, D. R. Stewart, *Nat. Nanotechnol.* **2013**, *8*, 13.

[3] Y. Yang, R. Huang, *Nat. Electron.* **2018**, *1*, 274.

[4] D. P. Sahu, S. N. Jammalamadaka, *Sci. Rep.* **2017**, *7*, 17224.

[5] Y. Yang, P. Gao, S. Gaba, T. Chang, X. Pan, W. Lu, *Nat. Commun.* **2012**, *3*, 732.

[6] S. H. Jo, T. Chang, I. Ebong, B. B. Bhadviya, P. Mazumder, W. Lu, *Nano Lett.* **2010**, *10*, 1297.

[7] L. Qi, L. Shibing, L. Hangbing, W. Wei, N. Jiebin, H. Zongliang, C. Junning, L. Ming, *ACS Nano* **2010**, *4*, 6162.

[8] C. Li, B. Gao, Y. Yao, X. Guan, X. Shen, Y. Wang, P. Huang, L. Liu, X. Liu, J. Li, C. Gu, J. Kang, R. Yu, *Adv. Mater.* **2017**, *29*, 1602976.

[9] B. G. Chae, J. B. Seol, J. H. Song, K. Baek, S. H. Oh, H. Hwang, C. G. Park, *Adv. Mater.* **2017**, *29*, 1701752.

[10] J. Zheng, J. Zhang, Z. Wang, L. Zhong, Y. Sun, Z. Liang, Y. Li, L. Jiang, X. Chen, L. Chi, *Adv. Mater.* **2018**, *30*, 1802731.

[11] H. Tan, G. Liu, H. Yang, X. Yi, L. Pan, J. Shang, S. Long, M. Liu, Y. Wu, R.-W. Li, *ACS Nano* **2017**, *11*, 11298.

[12] K. Pei, X. Ren, Z. Zhou, Z. Zhang, X. Ji, P. K. L. Chan, *Adv. Mater.* **2018**, *30*, 1706647.

[13] J. Gorecki, V. Apostolopoulos, J. Y. Ou, S. Mailis, N. Papasimakis, *Acs Nano* **2018**, *12*, 5940.

[14] Y. Shen, N. C. Harris, S. Skirlo, M. Prabhu, T. Baehr-Jones, M. Hochberg, X. Sun, S. Zhao, H. Larochelle, D. Englund, M. Soljačić, *Nat. Photonics* **2017**, *11*, 441.

[15] Z. Cheng, C. Ríos, W. H. P. Pernice, C. D. Wright, H. Bhaskaran, *Sci. Adv.* **2017**, *3*, 1700160.

[16] W. Xu, H. Cho, Y. H. Kim, Y. T. Kim, C. Wolf, C. G. Park, T. W. Lee, *Adv. Mater.* **2016**, *28*, 5916.

[17] B. Gholipour, P. Bastock, C. Craig, K. Khan, D. Hewak, C. Soci, *Adv. Optical Mater.* **2015**, *3*, 635.

[18] D. Xiang, T. Liu, J. Xu, J. Y. Tan, Z. Hu, B. Lei, Y. Zheng, J. Wu, A. H. C. Neto, L. Liu, W. Chen, *Nat. Commun.* **2018**, *9*, 2966.

[19] Y. Zhai, J.-Q. Yang, Y. Zhou, J. Mao, Y. Ren, V. A. L. Roy, S.-T. Han, *Mater. Horiz.* **2018**, *5*, 641.

[20] B. Gao, Y. Bi, H.-Y. Chen, R. Liu, P. Huang, B. Chen, L. Liu, X. Liu, S. Yu, H. S. P. Wong, J. Kang, *ACS Nano* **2014**, *8*, 6998.

[21] C. Wu, T. W. Kim, H. Y. Choi, D. B. Strukov, J. J. Yang, *Nat. Commun.* **2017**, *8*, 752.

[22] P. Russo, M. Xiao, R. Liang, N. Y. Zhou, *Adv. Electron. Mater.* **2018**, *28*, 1706230.

[23] H. Tan, G. Liu, X. Zhu, H. Yang, B. Chen, X. Chen, J. Shang, W. D. Lu, Y. Wu, R. W. Li, *Adv. Mater.* **2015**, *27*, 2797.

[24] K. A. Paller, A. D. Wagner, *Trends Cogn. Sci.* **2002**, *6*, 93.

[25] L. Q. Zhu, C. J. Wan, L. Q. Guo, Y. Shi, Q. Wan, *Nat. Commun.* **2014**, *5*, 3158.

[26] Z. Wang, S. Joshi, S. E. Savel'ev, H. Jiang, R. Midya, P. Lin, M. Hu, N. Ge, J. P. Strachan, Z. Li, Q. Wu, M. Barnell, G. L. Li, H. L. Xin, R. S. Williams, Q. Xia, J. J. Yang, *Nat. Mater.* **2017**, *16*, 101.

[27] H. Tian, W. Mi, H. Zhao, M. A. Mohammad, Y. Yang, P. W. Chiu, T. L. Ren, *Nanoscale* **2017**, *9*, 9275.

[28] C. Du, W. Ma, T. Chang, P. Sheridan, W. D. Lu, *Adv. Funct. Mater.* **2015**, *25*, 4290.

[29] L. Fenno, O. Yizhar, K. Deisseroth, *Annu. Rev. Neurosci.* **2011**, *34*, 389.

[30] O. Yizhar, L. E. Fenno, T. J. Davidson, M. Mogri, K. Deisseroth, *Neuron* **2011**, *71*, 9.

[31] B. L. Sinnen, A. B. Bowen, J. S. Forte, B. G. Hiester, K. C. Crosby, E. S. Gibson, M. L. Dell'Acqua, M. J. Kennedy, *Neuron* **2017**, *93*, 646.

[32] X. Liu, S. Ramirez, P. T. Pang, C. B. Puryear, A. Govindarajan, K. Deisseroth, S. Tonegawa, *Nature* **2012**, *484*, 381.

[33] K. Deisseroth, *Nat. Methods* **2011**, *8*, 26.

[34] X. Zhu, W. D. Lu, *ACS Nano* **2018**, *12*, 1242.

[35] Z. H. Tan, R. Yang, K. Terabe, X. B. Yin, X. D. Zhang, X. Guo, *Adv. Mater.* **2016**, *28*, 377.

[36] A. Rani, D. B. Velusamy, F. Marques Mota, Y. H. Jang, R. H. Kim, C. Park, D. H. Kim, *Adv. Funct. Mater.* **2017**, *27*, 1604604.

[37] Y. Shi, X. Liang, B. Yuan, V. Chen, H. Li, F. Hui, Z. Yu, F. Yuan, E. Pop, H. S. P. Wong, M. Lanza, *Nat. Electron.* **2018**, *1*, 458.

[38] J. Lee, W. D. Lu, *Adv. Mater.* **2018**, *30*, 1702770.

[39] L. Zhou, J. Mao, Y. Ren, S. T. Han, V. A. L. Roy, Y. Zhou, *Small* **2018**, *14*, 1703126.

[40] R. Waser, R. Dittmann, G. Staikov, K. Szot, *Adv. Mater.* **2009**, *21*, 2632.

[41] W. Lee, Y. Kim, Y. Song, K. Cho, D. Yoo, H. Ahn, K. Kang, T. Lee, *Adv. Funct. Mater.* **2018**, *28*, 1801162.

[42] M. A. Zidan, J. P. Strachan, W. D. Lu, *Nat. Electron.* **2018**, *1*, 22.

[43] J. H. Yoon, Z. Wang, K. M. Kim, H. Wu, V. Ravichandran, Q. Xia, C. S. Hwang, J. J. Yang, *Nat. Commun.* **2018**, *9*, 417.

[44] H. Ling, M. Yi, M. Nagai, L. Xie, L. Wang, B. Hu, W. Huang, *Adv. Mater.* **2017**, *29*, 1701333.

[45] M. D. Tran, H. Kim, J. S. Kim, M. H. Doan, T. K. Chau, Q. A. Vu, J.-H. Kim, Y. H. Lee, *Adv. Mater.* **2018**, *31*, 1807075.

[46] K. A. Mazzio, C. K. Luscombe, *Chem. Soc. Rev.* **2015**, *44*, 78.

[47] Z. Xiao, Y. Yuan, Y. Shao, Q. Wang, Q. Dong, C. Bi, P. Sharma, A. Gruverman, J. Huang, *Nat. Mater.* **2015**, *14*, 193.

[48] V. Adinolfi, E. H. Sargent, *Nature* **2017**, *542*, 324.

[49] S. Gao, G. Liu, H. Yang, C. Hu, Q. Chen, G. Gong, W. Xue, X. Yi, J. Shang, R.-W. Li, *ACS Nano* **2019**, *13*, 2634.

[50] A. Bera, H. Peng, J. Lourembam, Y. Shen, X. W. Sun, T. Wu, *Adv. Funct. Mater.* **2013**, *23*, 4977.

[51] M. Ungureanu, R. Zazpe, F. Golmar, P. Stoliar, R. Llopis, F. Casanova, L. E. Hueso, *Adv. Mater.* **2012**, *24*, 2496.

[52] D. S. Shang, J. R. Sun, L. Shi, B. G. Shen, *Appl. Phys. Lett.* **2008**, *93*, 102106.

[53] O. S. Game, G. J. Buchsbaum, Y. Zhou, N. P. Padture, A. I. Kingon, *Adv. Funct. Mater.* **2017**, *27*, 1606584.

[54] X. Guan, W. Hu, M. A. Haque, N. Wei, Z. Liu, A. Chen, T. Wu, *Adv. Funct. Mater.* **2018**, *28*, 1704665.

[55] L. Zhou, J. Y. Mao, Y. Ren, J. Q. Yang, S. R. Zhang, Y. Zhou, Q. Liao, Y. J. Zeng, H. Shan, Z. Xu, J. Fu, Y. Wang, X. Chen, Z. Lv, S. T. Han, V. A. L. Roy, *Small* **2018**, *14*, 1800288.

[56] X. Zhu, J. Lee, W. D. Lu, *Adv. Mater.* **2017**, *29*, 1700527.

[57] J. Choi, S. Park, J. Lee, K. Hong, D. H. Kim, C. W. Moon, G. D. Park, J. Suh, J. Hwang, S. Y. Kim, H. S. Jung, N. G. Park, S. Han, K. T. Nam, H. W. Jang, *Adv. Mater.* **2016**, *28*, 6562.

[58] Y. Wang, J. Yang, Z. Wang, J. Chen, Q. Yang, Z. Lv, Y. Zhou, Y. Zhai, Z. Li, S. T. Han, *Small* **2019**, *15*, 1805431.

[59] H. Fang, W. Hu, *Adv. Sci.* **2017**, *4*, 1700323.

[60] M. Wang, S. Cai, C. Pan, C. Wang, X. Lian, Y. Zhuo, K. Xu, T. Cao, X. Pan, B. Wang, S.-J. Liang, J. J. Yang, P. Wang, F. Miao, *Nat. Electron.* **2018**, *1*, 130.

[61] H. Zhang, *ACS Nano* **2015**, *9*, 9451.

[62] Y. Zhai, X. Yang, F. Wang, Z. Li, G. Ding, Z. Qiu, Y. Wang, Y. Zhou, S. T. Han, *Adv. Mater.* **2018**, *30*, 1803563.

[63] X. Zhou, Q. Zhang, L. Gan, H. Li, T. Zhai, *Adv. Funct. Mater.* **2016**, *26*, 4405.

[64] S. Bertolazzi, D. Krasnozhon, A. Kis, *ACS Nano* **2013**, *7*, 3246.

[65] Q. A. Vu, Y. S. Shin, Y. R. Kim, V. L. Nguyen, W. T. Kang, H. Kim, D. H. Luong, I. M. Lee, K. Lee, D. S. Ko, J. Heo, S. Park, Y. H. Lee, W. J. Yu, *Nat. Commun.* **2016**, *7*, 12725.

[66] J. Lee, S. Pak, Y. W. Lee, Y. Cho, J. Hong, P. Giraud, H. S. Shin, S. M. Morris, J. I. Sohn, S. Cha, J. M. Kim, *Nat. Commun.* **2017**, *8*, 14734.

[67] Z. Lv, Y. Wang, Z. Chen, L. Sun, J. Wang, M. Chen, Z. Xu, Q. Liao, L. Zhou, X. Chen, J. Li, K. Zhou, Y. Zhou, Y.-J. Zeng, S.-T. Han, V. A. L. Roy, *Adv. Sci.* **2018**, *5*, 1800714.

[68] Y. Wang, Z. Lv, Q. Liao, H. Shan, J. Chen, Y. Zhou, L. Zhou, X. Chen, V. A. L. Roy, Z. Wang, Z. Xu, Y. J. Zeng, S. T. Han, *Adv. Mater.* **2018**, *30*, 1800327.

[69] J. Xu, X. Zhao, Z. Wang, H. Xu, J. Hu, J. Ma, Y. Liu, *Small* **2019**, *15*, 1803970.

[70] Y. Zhou, S.-T. Han, X. Chen, F. Wang, Y.-B. Tang, V. A. L. Roy, *Nat. Commun.* **2014**, *5*, 4720.

[71] Q. Yan, Z. Luo, K. Cai, Y. Ma, D. Zhao, *Chem. Soc. Rev.* **2014**, *43*, 4199.

[72] M. A. Tasdelen, Y. Yagci, *Angew. Chem. Int. Edit.* **2013**, *52*, 5930.

[73] X. Chen, X. Zhu, S.-R. Zhang, J. Pan, P. Huang, C. Zhang, G. Ding, Y. Zhou, K. Zhou, V. A. L. Roy, S.-T. Han, *Adv. Mater. Technol.* **2018**, *4*, 1800551.

[74] X. Zhao, Z. Wang, Y. Xie, H. Xu, J. Zhu, X. Zhang, W. Liu, G. Yang, J. Ma, Y. Liu, *Small* **2018**, *14*, 1801325.

[75] Q. Zhang, J. He, H. Zhuang, H. Li, N. Li, Q. Xu, D. Chen, J. Lu, *Adv. Funct. Mater.* **2016**, *26*, 146.

[76] Q.-D. Ling, Y. Song, S.-L. Lim, E. Y.-H. Teo, Y.-P. Tan, C. Zhu, D. S. H. Chan, D.-L. Kwong, E.-T. Kang, K.-G. Neoh, *Angew. Chem. Int. Edit.* **2006**, *118*, 3013.

[77] S. Miao, H. Li, Q. Xu, Y. Li, S. Ji, N. Li, L. Wang, J. Zheng, J. Lu, *Adv. Mater.* **2012**, *24*, 6210.

[78] P.-Y. Gu, F. Zhou, J. Gao, G. Li, C. Wang, Q.-F. Xu, Q. Zhang, J.-M. Lu, *J. Am. Chem. Soc.* **2013**, *135*, 14086.

[79] B. Sun, M. Tang, J. Gao, C. M. Li, *Chem. Electro. Chem.* **2016**, *3*, 896.

[80] C.-L. Liu, W.-C. Chen, *Polym. Chem-UK* **2011**, *2*, 2169.

[81] C. Ye, Q. Peng, M. Li, J. Luo, Z. Tang, J. Pei, J. Chen, Z. Shuai, L. Jiang, Y. Song, *J. Am. Chem. Soc.* **2012**, *134*, 20053.

[82] Y. Li, H. Li, J. He, Q. Xu, N. Li, D. Chen, J. Lu, *Chem - Asian J.* **2016**, *11*, 2078.

[83] M. Irie, *Chem. Rev.* **2000**, *100*, 1685.

[84] M. Irie, T. Fukaminato, T. Sasaki, N. Tamai, T. Kawai, *Nature* **2002**, *420*, 759.

[85] H. Ling, K. Tan, Q. Fang, X. Xu, H. Chen, W. Li, Y. Liu, L. Wang, M. Yi, R. Huang, Y. Qian, L. Xie, W. Huang, *Adv. Electron. Mater.* **2017**, *3*, 1600416.

[86] Y. L. Kim, H. Y. Jung, S. Park, B. Li, F. Liu, J. Hao, Y.-K. Kwon, Y. J. Jung, S. Kar, *Nat. Photonics* **2014**, *8*, 239.

[87] Y. Wu, Y. Wei, Y. Huang, F. Cao, D. Yu, X. Li, H. Zeng, *Nano Res.* **2016**, *10*, 1584.

[88] Z. Sun, E. Ambrosi, A. Bricalli, D. Ielmini, *Adv. Mater.* **2018**, *30*, 1802554.

[89] K. Mathieson, J. Loudin, G. Goetz, P. Huie, L. Wang, T. I. Kamins, L. Galambos, R. Smith, J. S. Harris, A. Sher, D. Palanker, *Nat. Photonics* **2012**, *6*, 391.

[90] C. Choi, M. K. Choi, S. Liu, M. S. Kim, O. K. Park, C. Im, J. Kim, X. Qin, G. J. Lee, K. W. Cho, M. Kim, E. Joh, J. Lee, D. Son, S.-H. Kwon, N. L. Jeon, Y. M. Song, N. Lu, D.-H. Kim, *Nat. Commun.* **2017**, *8*, 1664.

[91] S. Chen, Z. Lou, D. Chen, G. Shen, *Adv. Mater.* **2018**, *30*, 1705400.

[92] W. Wu, X. Wang, X. Han, Z. Yang, G. Gao, Y. Zhang, J. Hu, Y. Tan, A. Pan, C. Pan, *Adv. Mater.* **2019**, *31*, 1805913.

[93] J. Lee, B. Yoo, H. Lee, G. D. Cha, H. S. Lee, Y. Cho, S. Y. Kim, H. Seo, W. Lee, D. Son, M. Kang, H. M. Kim, Y. I. Park, T. Hyeon, D. H. Kim, *Adv. Mater.* **2017**, *29*, 1603169.

[94] H. Wang, H. Liu, Q. Zhao, Z. Ni, Y. Zou, J. Yang, L. Wang, Y. Sun, Y. Guo, W. Hu, Y. Liu, *Adv. Mater.* **2017**, *29*, 1701772.

[95] L. Hu, S. Fu, Y. Chen, H. Cao, L. Liang, H. Zhang, J. Gao, J. Wang, F. Zhuge, *Adv. Mater.* **2017**, *29*, 1606927.

[96] S. Chen, A. Z. Weitemier, X. Zeng, L. He, X. Wang, Y. Tao, A. J. Y. Huang, Y. Hashimotodani, M. Kano, H. Iwasaki, L. K. Parajuli, S. Okabe, D. B. L. Teh, A. H. All, I. Tsutsui-Kimura, K. F. Tanaka, X. Liu, T. J. McHugh, *Science* **2018**, *359*, 679.

[97] Z. Wang, M. Hu, X. Ai, Z. Zhang, B. Xing, *Adv. Biosys.* **2019**, *3*, 1800233.

[98] T. Kyung, S. Lee, J. E. Kim, T. Cho, H. Park, Y. M. Jeong, D. Kim, A. Shin, S. Kim, J. Baek, J. Kim, N. Y. Kim, D. Woo, S. Chae, C. H. Kim, H. S. Shin, Y. M. Han, D. Kim, W. D. Heo, *Nat. Biotechnol.* **2015**, *33*, 1092.

[99] R. S. Zucker, W. G. Regehr, *Annu. Rev. Physiol.* **2002**, *64*, 355.

[100] D. E. Clapham, *Cell* **2007**, *131*, 1047.

[101] M. K. Kim, J. S. Lee, *ACS Nano* **2018**, *12*, 1680.

[102] J.-Y. Mao, L. Zhou, Y. Ren, J.-Q. Yang, C.-L. Chang, H.-C. Lin, H.-H. Chou, S.-R. Zhang, Y. Zhou, S.-T. Han, *J. Mater. Chem. C* **2019**, *7*, 1491.

[103] J. Sun, S. Oh, Y. Choi, S. Seo, M. J. Oh, M. Lee, W. B. Lee, P. J. Yoo, J. H. Cho, J.-H. Park, *Adv. Funct. Mater.* **2018**, *28*, 1804397.

[104] J.-Y. Mao, L. Hu, S.-R. Zhang, Y. Ren, J.-Q. Yang, L. Zhou, Y.-J. Zeng, Y. Zhou, S.-T. Han, *J. Mater. Chem. C* **2019**, *7*, 48.

[105] T. Tuma, A. Pantazi, M. Le Gallo, A. Sebastian, E. Eleftheriou, *Nat. Nanotechnol.* **2016**, *11*, 693.

[106] H. S. P. Wong, S. Raoux, S. Kim, J. Liang, J. P. Reifenberg, B. Rajendran, M. Asheghi, K. E. Goodson, *P. IEEE* **2010**, *98*, 2201.

[107] D. C. Hu, R. Yang, L. Jiang, X. Guo, *ACS Appl. Mater. Inter.* **2018**, *10*, 6463.

[108] M. Kumar, S. Abbas, J. Kim, *ACS Appl. Mater. Inter.* **2018**, *10*, 34370.

[109] S. Wang, C. Chen, Z. Yu, Y. He, X. Chen, Q. Wan, Y. Shi, D. W. Zhang, H. Zhou, X. Wang, P. Zhou, *Adv. Mater.* **2019**, *31*, 1806227.

[110] L. Qian, Y. Sun, M. Wu, C. Li, D. Xie, L. Ding, G. Shi, *Nanoscale* **2018**, *10*, 6837.

[111] Z. Xiao, J. Huang, *Adv. Electron. Mater.* **2016**, *2*, 1600100.

[112] H. Tian, Q. Guo, Y. Xie, H. Zhao, C. Li, J. J. Cha, F. Xia, H. Wang, *Adv. Mater.* **2016**, *28*, 4991.

[113] M. Lee, W. Lee, S. Choi, J. W. Jo, J. Kim, S. K. Park, Y. H. Kim, *Adv. Mater.* **2017**, *29*, 1700951.

[114] S. Qin, F. Wang, Y. Liu, Q. Wan, X. Wang, Y. B. Xu, S. Yi, X. Wang, Z. Rong, *2D Mater.* **2017**, *4*, 035022.

[115] S. Dai, X. Wu, D. Liu, Y. Chu, K. Wang, B. Yang, J. Huang, *ACS Appl. Mater. Inter.* **2018**, *10*, 21472.

[116] X. Wu, Y. Chu, R. Liu, H. E. Katz, J. Huang, *Adv. Sci.* **2017**, *4*, 1700442.

[117] R. A. John, F. Liu, N. A. Chien, M. R. Kulkarni, C. Zhu, Q. Fu, A. Basu, Z. Liu, N. Mathews, *Adv. Mater.* **2018**, *30*, 1800220.

[118] K. Wang, S. Dai, Y. Zhao, Y. Wang, C. Liu, J. Huang, *Small* **2019**, *15*, 1900010.

[119] Y. Chen, Y. Chu, X. Wu, W. Ou-Yang, J. Huang, *Adv. Mater.* **2017**, *29*, 1704062.

[120] X. Yan, Y. Pei, H. Chen, J. Zhao, Z. Zhou, H. Wang, L. Zhang, J. Wang, X. Li, C. Qin, G. Wang, Z. Xiao, Q. Zhao, K. Wang, H. Li, D. Ren, Q. Liu, H. Zhou, J. Chen, P. Zhou, *Adv. Mater.* **2018**, *31*, 1805284.

[121] S. Ham, S. Choi, H. Cho, S.-I. Na, G. Wang, *Adv. Funct. Mater.* **2019**, *29*, 1806646.

[122] G. Agnus, W. Zhao, V. Derycke, A. Filoramo, Y. Lhuillier, S. Lenfant, D. Vuillaume, C. Gamrat, J. P. Bourgoin, *Adv. Mater.* **2010**, *22*, 702.

[123] X. Yang, Y. Fang, Z. Yu, Z. Wang, T. Zhang, M. Yin, M. Lin, Y. Yang, Y. Cai, R. Huang, *Nanoscale* **2016**, *8*, 18897.

[124] M. Prezioso, F. Merrikh-Bayat, B. D. Hoskins, G. C. Adam, K. K. Likharev, D. B. Strukov, *Nature* **2015**, *521*, 61.

[125] Y. Lee, J. Y. Oh, W. Xu, O. Kim, T. R. Kim, J. Kang, Y. Kim, D. Son, J. B.-H. Tok, M. J. Park, Z. Bao, T.-W. Lee, *Sci. Adv.* **2018**, *4*, eaat7387.

[126] H. Wang, Q. Zhao, Z. Ni, Q. Li, H. Liu, Y. Yang, L. Wang, Y. Ran, Y. Guo, W. Hu, Y. Liu, *Adv. Mater.* **2018**, *30*, 1803961.

[127] H. E. Lee, J. H. Park, T. J. Kim, D. Im, J. H. Shin, D. H. Kim, B. Mohammad, I.-S. Kang, K. J. Lee, *Adv. Funct. Mater.* **2018**, *28*, 1801690.

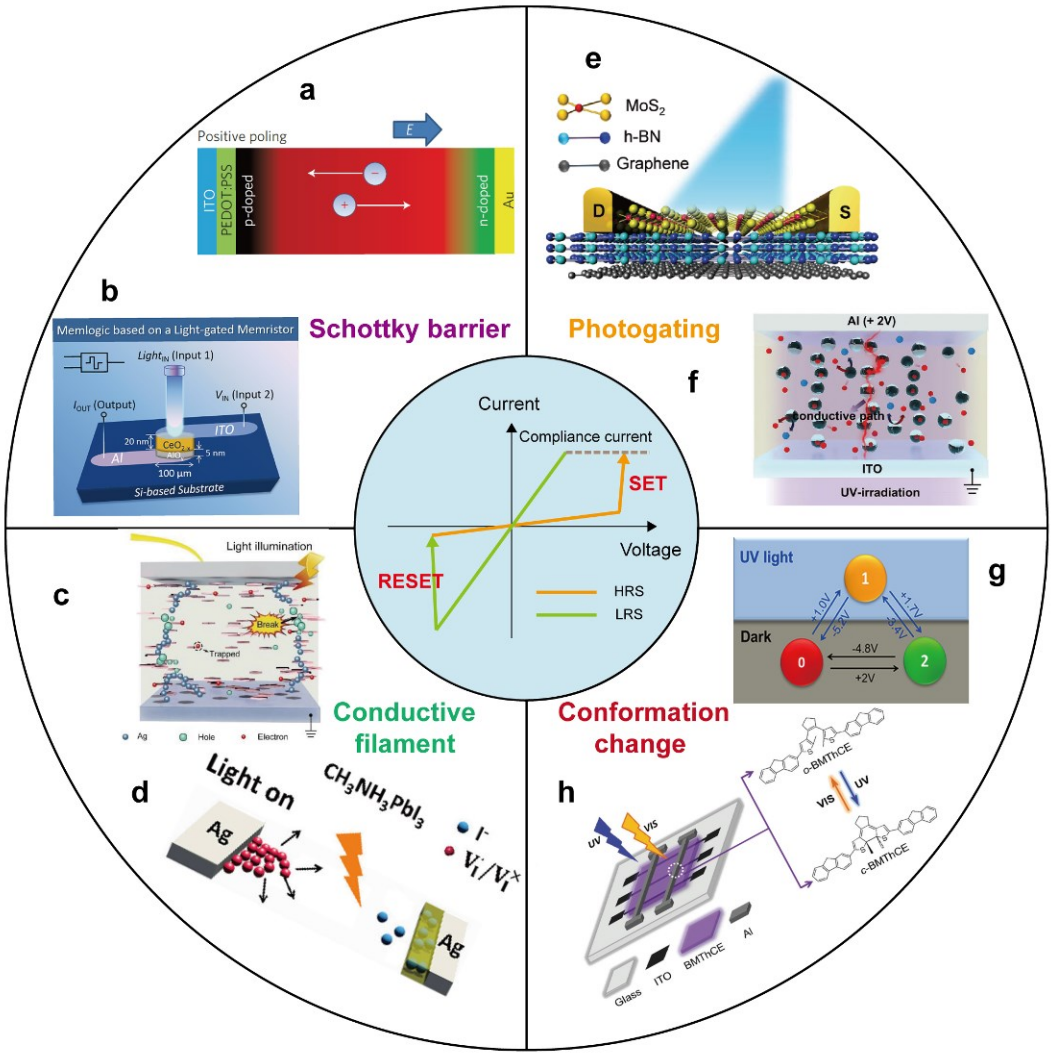

Figure 1. Physical mechanisms of photo-tunable resistive switching devices. a) Sketch diagrams of positively and negatively charged ion drift to the opposite direction in perovskite under positive bias, resulting in the p–i–n junction within $CH_3NH_3PbI_3$ film. Reproduced with permission.[47] Copyright 2014, Springer Nature. b) Schematics of a light gated memristor with a structure of ITO/CeO_{2-x}/AlO_y/Al. Reproduced with permission.[11] Copyright 2017, American Chemical Society. c) Rupture of conductive filament in $MoSe_2/Bi_2Se_3$ nanosheets film under NIR illumination. Reproduced with permission.[58] Copyright 2019, Wiley-VCH. d) Facilitated filament rupture in $CH_3NH_3PbI_3$ planar device under light illumination. Reproduced with permission.[34] Copyright 2018, American Chemical Society. e) Schematic diagram of the flash transistor-like structure of a MoS_2/h-BN/graphene heterostructure. Reproduced with permission.[45] Copyright 2018, Wiley-VCH. f) Formation of conductive path in carbon quantum dots-silk device. Reproduced with permission.[67] Copyright

2018, Wiley-VCH. g) Transitions among different resistance states and corresponding threshold voltages of donor–bridge–acceptor compound (DBA) memory device. Reproduced with permission.[81] Copyright 2012, American Chemical Society. h) Schematic illustration of the BMThCE-based memory device as well as the chemical structures of the light-induced transition between *o*-BMThCE and *c*-BMThCE. Reproduced with permission.[85] Copyright 2017, Wiley-VCH.

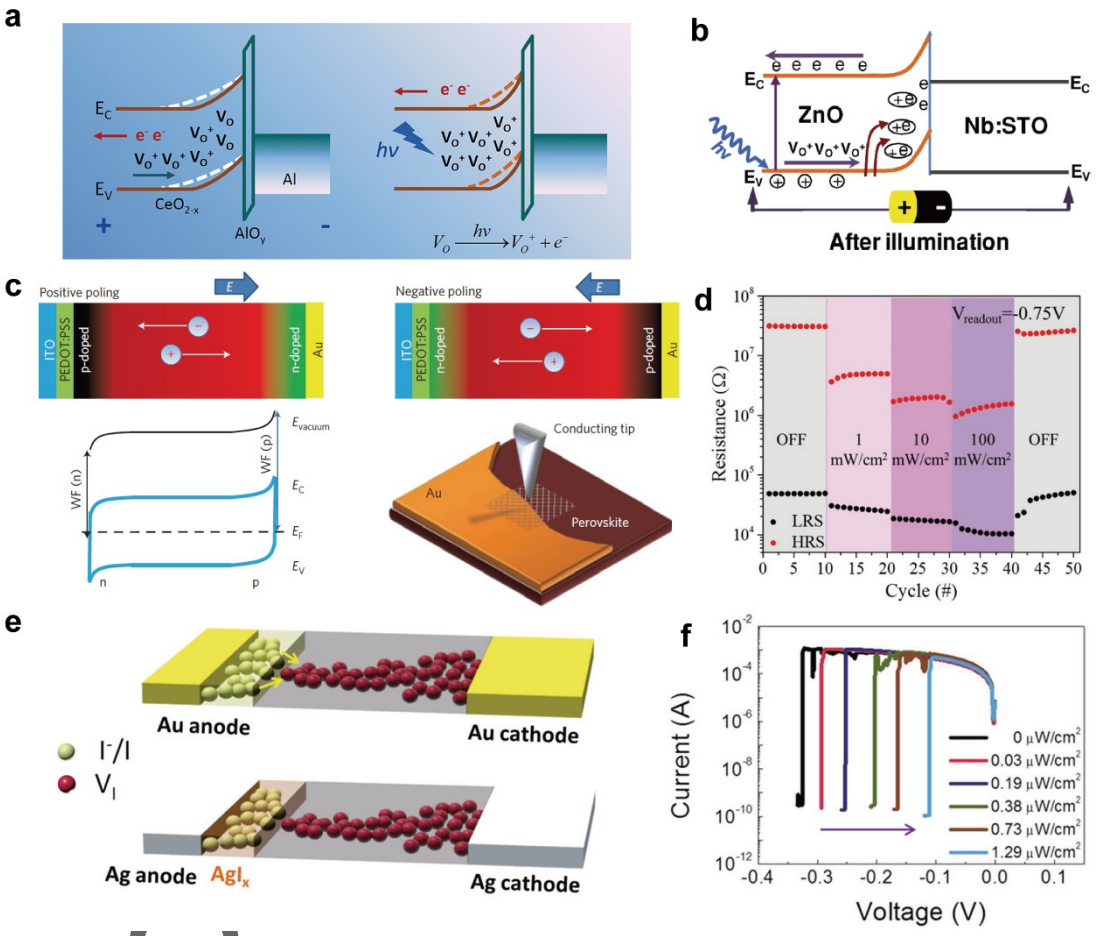

Figure 2. Photovoltaic effect-induced interfacial Schottky barrier and formation and annihilation of conductive filaments. a) Energy band diagram depicting the operation mechanism of electrical erasing and optical programing. Reproduced with permission.[11] Copyright 2017, American Chemical Society. b) Energy band diagram of the reversely biased heterojunction showing sustained photocurrent induced by charge separation process after the illumination of UV light. Reproduced with permission.[50] Copyright 2013, Wiley-VCH. c) Switchable photovoltaic model and mechanism study. Sketch diagrams of positively and negatively charged ion drift to the opposite direction in perovskite under positive and negative bias, resulting in the p–i–n junction (energy diagram). A section of Au electrode was removed for further KPFM potential measurements. Reproduced with permission.[47] Copyright 2014, Springer Nature. d) Light modulation on LRS and HRS with different

intensities. Reproduced with permission.[54] Copyright 2017, Wiley-VCH. e) Sketch of the conductive filament consisting of iodine vacancies in the planar configuration device. f) RESET process under broadband visible light with different light intensities. Reproduced with permission.[34] Copyright 2017, Wiley-VCH.

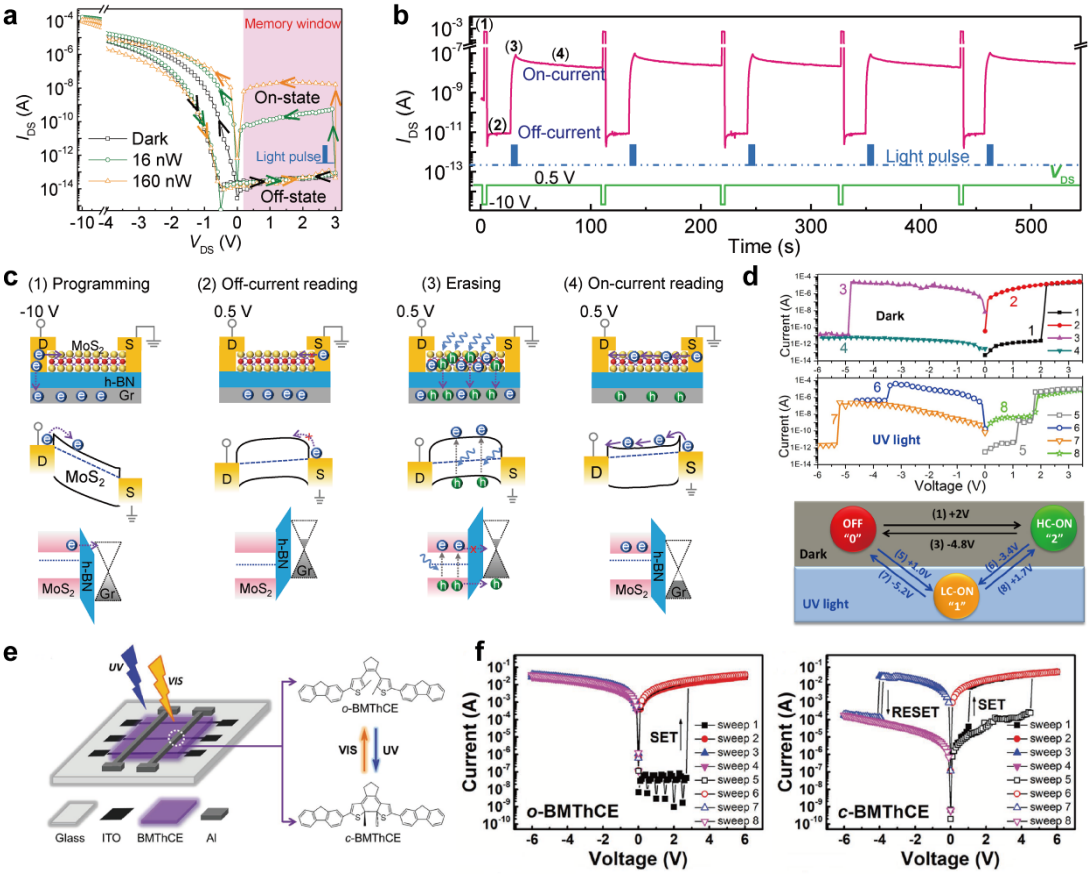

Figure 3. Photogating effect and photo-induced conformation change. a) *I*–*V* characteristics of the MoS_2/h-BN/graphene heterostructure optical flash memory. b) Reproducible programing and erasing cycles by electrical and optical pulses, respectively. c) Working mechanism of the optical memory. (1) Electrical programming by applying a -10 V bias to drain electrode. (2) Reading of ON state under dark condition by applying a 0.5 V bias. (3) Optical erasing for 1 s with a 458 nm laser. (4) Reading of OFF state under dark condition by applying a 0.5 V bias. Reproduced with permission.[45] Copyright 2018, Wiley-VCH. d) Different *I*–*V* characteristics and threshold voltages under dark and UV light illumination of donor–bridge–acceptor compound (DBA) memory device. Reproduced with permission.[81] Copyright 2012, American Chemical Society. e) Scheme of the BMThCE-based device as well as the chemical structures of the light-induced transition between *o*-BMThCE and *c*-BMThCE.

f) *I*–*V* curves of the memory devices based on *o*-BMThCE and *c*-BMThCE. Reproduced with permission.[85] Copyright 2017, Wiley-VCH.

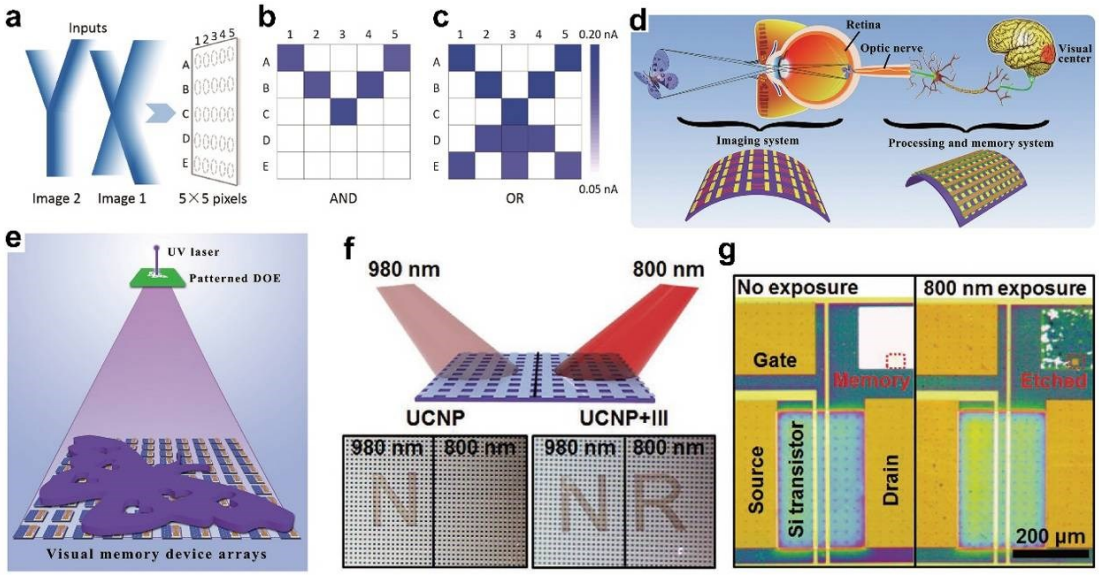

Figure 4. Memristor-involved photonic applications. a) Patterns "X" and "Y" fed into the memlogic devices; output sketch of b) the same regions and c) all the parts of both input patterns. Reproduced with permission.[11] Copyright 2017, American Chemical Society. d) Schematic illustrations of imaging and memory system corresponding to human visual memory. e) Schematic illustration of the detected and memorized image of the artificial visual memory. Reproduced with permission.[91] Copyright 2018, Wiley-VCH. f) Graphs depict the selective destruction of data under 980 and 800 nm laser illumination. The left side corresponds to the UCNPs with etched Mg layer while the one on the right side indicates the UCNPs with sensitizer III. g) Magnified image of the integrated device before (left) and after (right) 800 nm laser illumination. Reproduced with permission.[93] Copyright 2017, Wiley-VCH.

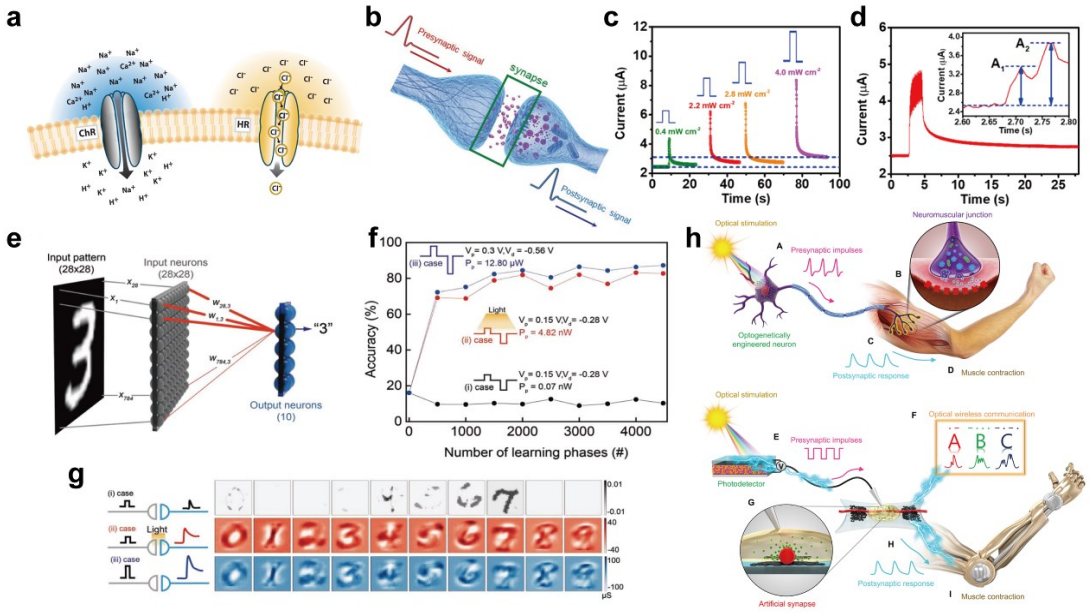

Figure 5. Light-tunable synaptic plasticity. a) Diagrams of ion conduction under light illumination in optogenetics. Reproduced with permission.[30] Copyright 2011, Elsevier Inc. b) Schematic of the connection between adjacent neurons (biological synapse). Reproduced with permission.[103] Copyright 2018, Wiley-VCH. c) Current response under the application of single light pulse with different incident light intensities (0.4, 2.2, 2.8 and 4.0 mW cm^{-2}); d) current response under the application a sequence of light pulses. The inset demonstrates the amplitude change of peak current after the application of two consecutive pulses. Reproduced with permission.[108] Copyright 2018, American Chemical Society. e) A single-layer artificial neural network is composed of 784 input and 10 output neurons, jointed by independent synapse with different synaptic weight. Each input neurons correspond to a pixel of the input pattern. f) Pattern recognition rate against the number of learning phases. g) Sketch images of eventual synaptic weights correlated to the input patterns for all the three training modes. Reproduced with permission.[121] Copyright 2018, Wiley-VCH. h) Biological and artificial synapse under optical simulation and the corresponding muscle response. Reproduced with permission.[125] Copyright 2018, AAAS.

TOC entry:

The development of photonic memristors and their application in photonic computing and emulation on optogenetics-modulated artificial synapses are reviewed. Photoactive materials as photo-sensing and storage media are discussed, considering their optical-tunable memory behavior and resistive switching mechanism including photogating and photovoltaic effect. Light-involved logic operations, system level integration and artificial synaptic memristors along with improved learning tasks performance are presented.

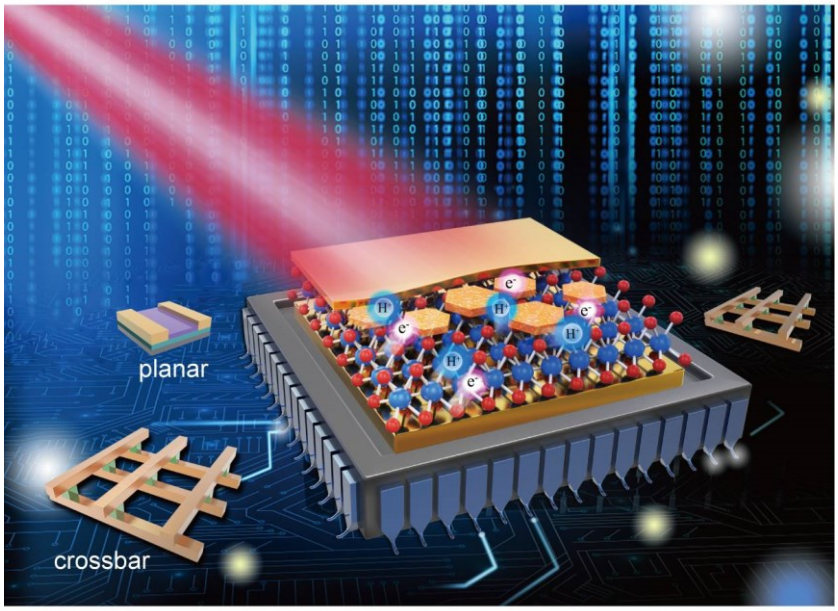

Jingyu Mao is currenly a postgraduate student in the Institute for Advanced Study, Shenzhen University, under the supervision of Prof. Ye Zhou. His research interests focus on the design and fabrication of memory devices including resistive switching memory and flash memory, as well as their application in articial neural networks.

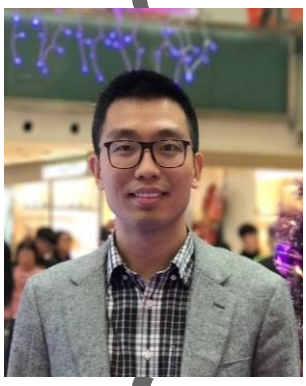

Ye Zhou is an IAS Fellow in the Institute for Advanced Study, Shenzhen University. His research interests include flexible and printed electronics, organic/inorganic semiconductors, surface and interface physics, nanostructured materials, and nano-scale devices for technological applications, such as logic circuits, data storage, energy harvesting, photonics and sensors.

Su-Ting Han is an associate professor at Shenzhen University and a visiting associate professor at The University of Michigan. She received her MSc degree in Analytical Chemistry from Hong Kong Baptist University and her PhD degree in Physics and Materials Science from City University of Hong Kong. Her research interests include functional electronic devices and flexible, stretchable, and wearable electronics.